Mon. Not. R. Astron. Soc. **354,** 457–465 (2004) doi:10.1111/j.1365-2966.2004.08205.x

A comparison of Rosseland-mean opacities from OP and OPAL

M. J. Seaton[1] and N. R. Badnell[2]★

[1]*Department of Physics and Astronomy, University College London, London WC1E 6BT*
[2]*Department of Physics, University of Strathclyde, Glasgow G4 0NG*

Accepted 2004 July 7. Received 2004 April 20

ABSTRACT

Monochromatic opacities from the Opacity Project (OP) have been augmented by hitherto missing inner-shell contributions. OP Rosseland-mean opacities, $\kappa_{\rm R}$, are compared with results from OPAL for the six elements H, He, C, O, S and Fe. The OPAL data are obtained from the project's website.

Agreement for H is close everywhere except for the region of $\log(T) \simeq 6$ and $\log(R) \simeq -1$ ($R = \rho/T_6^3$ where ρ is mass density in g cm^{-3} and $T_6 = 10^{-6} \times T$ with T in K). In that region $\kappa_{\rm R}$(OPAL) is larger than $\kappa_{\rm R}$(OP) by up to 13 per cent. The differences are caused by different equations of state (EOS). In the region concerned, OP has the H ground state undergoing dissolution, leading to a small H-neutral ionization fraction, while OPAL has larger values for that fraction. A similar difference occurs for He at $\log(R) \simeq -1$ and $\log(T) \simeq 6.4$, where OP has the He^+ ground state undergoing dissolution.

The OPAL website does not provide single-element Rosseland means for elements other than H and He. Comparisons between OP and OPAL are made for mixtures with $X = 0.9$, $Z = 0.1$ and Z containing pure C, O or S. There are some differences: at the lower temperatures, say $\log(T) \leqslant 5.5$, owing to differences in atomic data, with the OP R-matrix data probably being the more accurate; and at higher temperatures mainly owing to differences in level populations resulting from the use of different EOS theories.

In the original OP work, R-matrix data for iron were supplemented by data obtained using the configuration-interaction (CI) code SUPERSTRUCTURE. The experiment is made of replacing much of the original iron data with new data from the CI code AUTOSTRUCTURE. Inclusion of intercombination lines gives an increase in $\kappa_{\rm R}$ of up to 18 per cent.

The OPAL website does not allow for Z containing pure iron. Comparisons are made for an iron-rich mixture, $X = 0.9$, $Z = 0.1$ and Z containing C and Fe with C:Fe = 2:1 by number fraction. There are some differences between OP and OPAL for that case: the OP 'Z-bump' in $\kappa_{\rm R}$ is shifted to slightly higher temperatures, compared with OPAL.

Overall, there is good agreement between OP and OPAL Rosseland-mean opacities for the six elements, but there are some differences. Recent work has shown that helioseismology measurements give a very accurate value for the depth of the solar convective zone, $R_{\rm CZ}$, and that, taking account of recent revisions in abundances, solar models give agreement with that value only if opacities at $R_{\rm CZ}$ are about 20 per cent larger than OPAL values. For the six-element mix at $R_{\rm CZ}$ we obtain $\kappa_{\rm R}$(OP) to be larger than $\kappa_{\rm R}$(OPAL) by 5 per cent.

Key words: atomic processes – radiative transfer – stars: interiors.

1 INTRODUCTION

Rosseland-mean opacities from the Opacity Project (OP), as originally presented in Seaton et al. (1994), were in good agreement with those from the OPAL project (Rogers & Iglesias 1992a) over much of the temperature–density plane, but were smaller than those from OPAL at high temperatures and densities. Iglesias & Rogers (1996) offered the explanation that OP was missing some data for inner-shell transitions and that was confirmed in a recent paper by the present authors (Badnell & Seaton 2003). The results of Iglesias & Rogers (1996) and Badnell & Seaton (2003) were for a mixture of six elements: H, He, C, O, S and Fe, with abundances, by number fraction, given in Table 1. We refer to that as the six-element mix;

★E-mail: badnell@phys.strath.ac.uk

Table 1. The six-element mixture of Iglesias & Rogers 1996 and Badnell & Seaton 2003.

Element	Number fraction
H	9.071(−1)*
He	9.137(−2)
C	4.859(−4)
O	9.503(−4)
S	9.526(−5)
Fe	3.632(−5)

*$9.071(-1) = 9.071 \times 10^{-1}$.

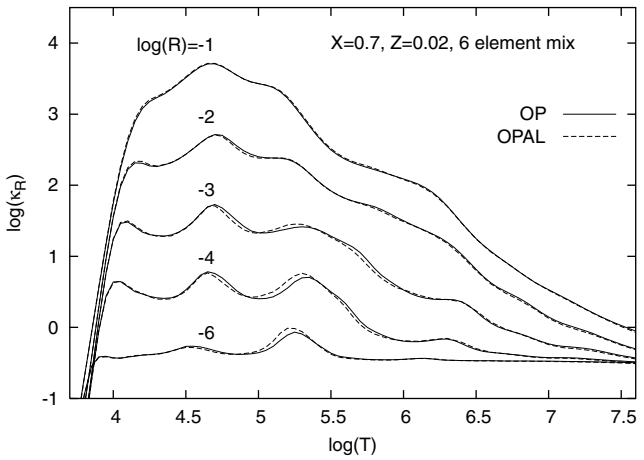

Figure 1. Comparisons of $\log(\kappa_R)$ from OP and OPAL for the six-element mixture of Table 1. OP from Badnell & Seaton (2003), OPAL from their website. Curves are labelled by values of $\log(R)$ where $R = \rho/T_6^3$, ρ is mass density in g cm^{-3} and T_6 is $10^6 \times T$ with T in K.

mass-fractions are $X = 0.7$ for H, $Y = 0.28$ for He, $Z = 0.02$ for 'metals'.

Fig. 1 shows the level of agreement between OP and OPAL, for that mix, as obtained in Badnell & Seaton (2003): values of $\log(\kappa_R)$, where κ_R is Rosseland-mean opacity in cm^2 g^{-1}, are plotted against $\log(T)$ for five different values of $\log(R)$ where $R = \rho/T_6^3$, $\rho =$ density in g cm^{-3} and $T_6 = 10^6 \times T$ with T in K [fig. 1 of Seaton et al. 1994 shows the behaviour of $\log(R)$ for a few typical stellar models]. The OPAL data are obtained from the OPAL website[1] and the OP data include the inner-shell contributions discussed in Badnell & Seaton (2003). It is seen that the agreement between OP and OPAL is fairly good in all cases but that there are some differences. The purpose of the present paper is to make more detailed comparisons of OP and OPAL for the six elements H, He, C, O, S and Fe. Work on the inclusion of OP inner-shell data for other elements is in progress.

2 ROSSELAND MEANS

Let $\sigma_k(u)$ be the cross-section for absorption or scattering of radiation by element k, where $u = h\nu/(k_B T)$, ν is frequency and k_B is Boltzmann's constant. For a mixture of elements with number fractions f_k, $\sum_k f_k = 1$, put $\sigma(u) = \sum_k f_k \sigma_k(u)$ (see Section 4.1).

[1] http://www-phys.llnl.gov/Research/OPAL/

The Rosseland-mean cross-section is σ_R, where

$$\frac{1}{\sigma_R} = \int_0^\infty \frac{F(u)}{\sigma(u)}\,\mathrm{d}u \tag{1}$$

and

$$F(u) = \left[\frac{15}{(4\pi^4)}\right] u^4 \exp(-u)/[1-\exp(-u)]^2. \tag{2}$$

The Rosseland-mean opacity per unit mass is $\kappa_R = \sigma_R/\mu$ where μ is mean molecular weight.

3 EQUATIONS OF STATE

The populations of the energy levels providing absorption or scattering of radiation are determined by the equation of state (EOS). OP and OPAL have very different treatments of the problem: the former use what is referred to as the 'chemical picture'; the latter the 'physical picture'.

3.1 The OP EOS

Let i be equal to the number of bound electrons in ionization stage i. In the OP work the *internal partition function* for stage i is taken to be (Hummer & Mihalas 1988)

$$U_i = \sum_j g_{ij} W_{ij} \exp[-E_{ij}/(k_B T)], \tag{3}$$

where j specifies an energy level, g_{ij} is a statistical weight, W_{ij} an *occupation probability* and E_{ij} the total energy of level ij. Let ϕ_i be the fraction of atoms in stage i. In the OP work (Hummer & Mihalas 1988; Seaton 1987a)

$$\frac{\phi_i}{\phi_{i-1}} = \frac{U_i}{U_{i-1}} \times \frac{N_e}{U_e}, \tag{4}$$

where

$$U_e = 2\left\{\frac{m_e k_B T}{2\pi\hbar^2}\right\}^{3/2} \tag{5}$$

and m_e is the electron mass. Allowance for electron degeneracy, and other refinements, is discussed in Graboske, Harwood & Rogers (1969) and in section IV(e) of Hummer & Mihalas (1988).

In the OP work, the W_{ij} are calculated using methods described in Hummer & Mihalas (1988) which are plausible but not rigorous (some modifications of the treatment in Hummer & Mihalas 1988 are discussed in Badnell & Seaton 2003). The OP W_{ij} become small for levels which are sufficiently highly excited (referred to as 'level dissolution'), which ensures convergence of the summation in (3). In many circumstances the Boltzmann factors in (3), $\exp[-E_{ij}/(k_B T)]$, become small long before there is a cut-off due to the W_{ij} becoming small: in those circumstances the calculated opacities are insensitive to the exact values of the W_{ij}.

3.2 The OPAL EOS

The OPAL approach to the EOS problems is based on the many-body quantum statistical mechanics of partially ionized plasmas (see Rogers 1981 and Rogers & Iglesias 1992b for a summary of later work). The level populations obtained by OPAL may be expressed in terms of the W factors of OP. Comparisons of results from OPAL and OP are given in Hummer (1988) for H and H^+ and in Iglesias & Rogers (1996) for hydrogenic C. It is found that, compared with OP, OPAL has larger populations in the more highly excited states.

The case of hydrogenic C was discussed further in Badnell & Seaton (2003) where it was found that OPAL gave W factors to be surprisingly large for states that had mean volumes larger than the mean volumes available per particle in the plasma.

4 OPACITIES FOR MIXTURES

In principle, the level populations for any one chemical element depend on the abundances of all other elements present in a plasma. However, it would not be practicable to make complete *ab initio* calculations of opacities for every mixture which may be of interest. Some approximations must therefore be made.

4.1 The OP approach

The OP W_{ij} depend on the ion microfield which should, of course, depend on the chemical mixture. The approximation is made of using a microfield independent of mixture (in practice, that for fully ionized H and He with $X = 0.7$, $Y = 0.3$). Monochromatic opacities are then calculated for each chemical element, as functions of frequency, on a grid of values of T and $N_{\rm e}$ [in practice, usually with intervals of $\delta \log(T) = 0.05$ and $\delta \log(N_{\rm e}) = 0.5$]. The monochromatic opacities are then simply added together for the calculation of Rosseland means for mixtures. In most cases that procedure does not lead to significant error, but there are exceptions (see, for example, Section 7.3).

4.2 The OPAL approach

The OPAL work makes use of interpolation procedures based on the concept of 'corresponding states' (see Rogers & Iglesias 1993). Rosseland-mean opacities are available from the OPAL website for 'metal' mass-fractions $Z \leqslant 0.1$. In general the use of interpolations does not introduce any important errors (see Rogers & Iglesias 1993) but there may be some significant errors near the edges of the domains of the tables provided.

5 ATOMIC PHYSICS

5.1 *R*-matrix calculations

Most of the atomic data used in the original OP work were obtained using the *R*-matrix method (RM; see Berrington et al. 1987). For a system containing N electrons we use the wavefunction expansion

$$\Psi = \mathcal{A} \sum_p \psi_p(\boldsymbol{x}_1, \ldots, \boldsymbol{x}_{N-1}) \times \theta_p(\boldsymbol{x}_N) + \sum_m \Phi_m(\boldsymbol{x}_1, \cdots, \boldsymbol{x}_N) \times c_m, \quad (6)$$

where: $\mathcal{A}$ is an anti-symmetrization operator; $\boldsymbol{x}_i$ is a space-and-spin coordinate for electron i; ψ_p is a function for a state k of the $(N-1)$-electron core (usually calculated using a configuration-interaction code); θ_p is an orbital function for an added electron; Φ_m is a function of bound-state type for the N-electron system; c_m is a coefficient. In the *R*-matrix method the functions θ_k and coefficients c_m are fully optimized.

Further details on the *R*-matrix calculations are given in Seaton et al. (1992) and by The Opacity Project Team (1995, 1997).

5.2 SUPERSTRUCTURE and AUTOSTRUCTURE

The configuration-interaction (CI) codes SUPERSTRUCTURE (SS; Eissner, Jones & Nussbaumer 1974) and AUTOSTRUCTURE (AS; Badnell 1987, 1997) use expansions

$$\Psi = \sum_m \Phi_m, \quad (7)$$

where the Φ_m are one-configuration functions. The code SS is used only for calculating energies of bound states and radiative transition probabilities: AS, which was developed from SS, includes calculations for autoionizing states, autoionization probabilities, and cross-sections for photoionization.

In using the CI codes for a level of a given configuration $\mathcal{C}$, we usually attempt to include in the expansion (7) at least all of the states belonging to the complex of which $\mathcal{C}$ is a member.

5.3 Methods used in OPAL

OPAL uses single-configuration wavefunctions,

$$\Psi = \Phi_m, \quad (8)$$

with one-electron orbitals calculated using potentials adjusted empirically such as to give best agreement with experimental energy-level data (Rogers, Wilson & Iglesias 1988; Iglesias, Rogers & Wilson 1992).

6 SPECTRUM LINES

Inclusion of contributions from large numbers of spectrum lines is of crucial importance.

6.1 Inclusion of lines

Our procedure is, first, to calculate the monochromatic opacity cross-section $\sigma(\nu)$ including only continuum processes (photoionization and detachment, free–free processes and scattering) and to determine a mean background $\sigma_{\rm B}(\nu)$ such that, at each frequency point ν, $\sigma(\nu) \geqslant \sigma_{\rm B}(\nu)$. Let $\sigma_{\rm L}(\nu)$ be the contribution from a spectral line. We define a quantity TESTL and, at each frequency mesh-point, include the line contribution if

$$\sigma_{\rm L}(\nu) \geqslant {\rm TESTL} \times \sigma_{\rm B}(\nu). \quad (9)$$

We take TESTL to be small (usually TESTL $= 10^{-8}$): the contribution from each line may be small but the number of lines may be very large.

6.2 Fine structure

Inclusion of the fine structures of the spectrum lines can lead to a redistribution of oscillator strength, which can give a significant increase in $\sigma_{\rm R}$ defined by (1). In the original OP work, fine structure was allowed for by methods described in Section 4.5 of Seaton et al. (1994): simple *LSJ*-coupling formulae were used together with empirical estimates of averaged spin–orbit parameters so as to determine level splittings. It was checked that the method was very stable, in that variation of the parameters over a wide range gave hardly any change in the calculated values of $\sigma_{\rm R}$. However, the method did not allow for the inclusion of intercombination (spin forbidden) lines, which can be important for highly ionized systems.

6.3 Line profiles

The quantity σ_R can be sensitive to the widths of the spectrum lines, which are caused by radiation damping, thermal Doppler effects and pressure broadening. Both OP and OPAL use similar empirical formulae for the pressure widths based on a theory originally proposed by Griem (1968). They differ in that OPAL adopts parameters determined from available experimental data (Dimitrijević & Konjević 1981) while OP uses results from ab initio calculations (Seaton 1987b, 1988; Burke 1992). In the fairly small number of cases for which direct comparisons have been made (Seaton 1988) the agreement between OP and OPAL pressure widths is very close.

It may be noted that σ_R is sensitive to pressure broadening only for intermediate values of the density: at sufficiently low densities the pressure widths are small compared with those arising from radiation damping and Doppler effects, while at high densities the lines are blended to form a quasi-continuum.

7 HYDROGEN AND HELIUM

The basic physical data for H and He (energy levels, radiative transition probabilities and cross-sections for photo-detachment, photoionization and free–free transitions) are known accurately, and theories of pressure broadening of lines for those elements are well developed and should be quite reliable. Fig. 2 gives OP and OPAL results for a H/He mixture with mass fractions of $X = 0.7$ for H and $Y = 0.3$ for He. As is to be expected, the agreement between OP and OPAL is generally very close but there is a region with some differences for $\log(R) = -1$ within the vicinity of $\log(T) = 6$. We discuss that region further.

7.1 Hydrogen

The top part of Fig. 3 shows $\log(\kappa_R)$ for pure H with $\log(R) = -1$ and $\log(T) = 5$ to 7, and the lower part shows the first derivative,

$$\partial \log(\kappa_R)/\partial \log(T), \tag{10}$$

calculated in the approximation of using first differences. The largest difference between OP and OPAL occurs for $\log(T) \simeq 6.0$ and in that region there is a marked change in the behaviour of $\partial \log(\kappa_R)/\partial \log(T)$, which becomes practically constant for $\log(T) > 6.5$. There are three main contributions to hydrogen opacities in the region considered: (1) scattering of photons by free

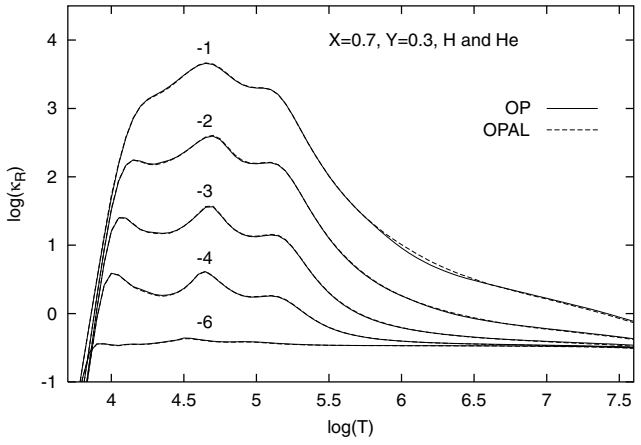

Figure 2. Comparisons of $\log(\kappa_R)$ from OP and OPAL for a H/He mixture with mass fractions $X = 0.7$ for H and $Y = 0.3$ for He. Curves are labelled by values of $\log(R)$.

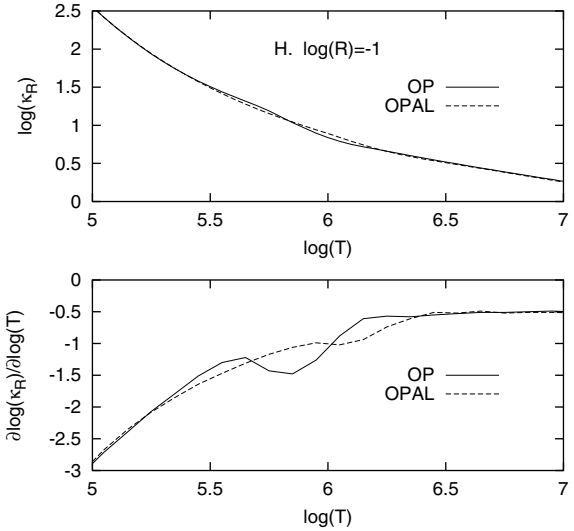

Figure 3. Upper figure: $\log(\kappa_R)$ for pure H, $\log(R) = -1$, $\log(T) = 5$ to 7. Lower figure: the derivative $\partial \log(\kappa_R)/\partial \log(T)$ calculated using first differences.

electrons; (2) electron–proton free–free transitions; (3) hydrogen bound–free transitions. Contributions from (3) become very small for $\log(T)$ significantly larger than 6.0, as H becomes fully ionized.

OP calculations are first made on a mesh of values of [$\log(T)$, $\log(N_e)$] and interpolations to required values of [$\log(T)$, $\log(\rho)$] are then made using the code OPFIT.F Seaton (1993). Table 2 gives results for the hydrogen ionization equilibria at $\log(T) = 6.0$: values of $\log(R)$; values of $\log(N_e)$; $\phi(1)$ (fraction of neutral H); and $W(1)$ (H ground-state occupation probability) from OP. The table also includes values of $\log(N_e)$ and $\phi(1)$ from OPAL (data kindly supplied by Dr C. A. Iglesias). The trends for OP may be described as follows: with increasing density, $\phi(1)$ initially increases owing to the factor N_e/U_e in (3) (pressure recombination) but for the larger values of density $W(1)$ becomes small leading to smaller values of $\phi(1)$ (pressure ionization). The values of $\phi(1)$ from OPAL are much larger than those from OPAL and the additional amount of neutral H explains the difference between the OP and OPAL opacities.

It will be noted that at the lower densities of Table 2 the values of $\phi(1)$ from OPAL continue to be larger than those from OP. The reason is that the OPAL values of the $W(n)$ for $n > 1$ are larger than the OP values. However, those differences in ionization equilibria at the lower densities do not have much effect on the Rosseland-mean opacities.

Table 2. Hydrogen ionization equilibria at $\log(T) = 6.0$.

	OP			OPAL	
$\log(R)$	$\log(N_e)$	$\phi(1)$	$W(1)$	$\log(N_e)$	$\phi(1)$
−2.776	21.00	5.304(−4)	0.960	21.00	1.090(−2)
−2.276	21.50	1.324(−3)	0.863	21.49	1.506(−2)
−1.775	22.00	2.689(−3)	0.575	22.00	2.101(−2)
−1.276	22.50	2.751(−3)	0.190	22.49	2.546(−2)
−0.776	23.00	1.491(−3)	0.034	22.98	4.164(−2)
−0.276	23.50	6.424(−4)	0.005	23.45	1.069(−1)

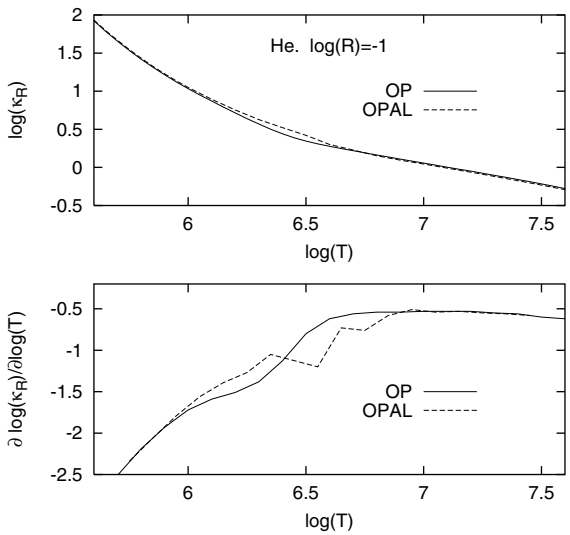

Figure 4. Upper figure: $\log(\kappa_{\rm R})$ for pure He, $\log(R) = -1$, $\log(T) = 5.7$ to 7.5. Lower figure: the derivative $\partial \log(\kappa_{\rm R})/\partial \log(T)$ calculated using first differences.

7.2 Helium

Fig. 4, for helium, shows results similar to those of Fig. 3 for hydrogen. At $\log(R) = -1$ the maximum difference between the OP and OPAL opacities occurs for $\log(T) \simeq 6.4$. That is the region where the OP occupation probability for the He^+ ground state becomes small. The OPAL populations for He^+ will be much larger than those from OP.

7.3 Smoothness

A further feature of Figs 3 and 4 may be noted. Both OP and OPAL give rise to somewhat irregular appearances for the derivatives $\log(\kappa_{\rm R})/\log(T)$. Dr Iglesias informs us that when producing a pure H or He table for OPAL it is necessary to do some interpolating, which might explain the irregularities in the OPAL data. The OP work also involves interpolations. A check run was made for H using intervals of $\delta \log(T) = 0.025$ and $\delta \log(N_{\rm e}) = 0.25$, that is to say one half of those normally used, and it was found to give close agreement with the results presented in Fig. 3.

7.4 Summary on H and He

The differences between OP and OPAL for level populations (and, more generally, for equations of state, EOS) have been discussed in a number of previous papers (Hummer 1988; Iglesias & Rogers 1996; Badnell & Seaton 2003) and will not be discussed further here. Our present concern is only with effects on opacities. For pure H and pure He the largest differences in opacities, at $\log(R) = -1$, are 13 per cent for H at $\log(T) = 6.0$ and 20 per cent for He at $\log(T) = 6.4$. For smaller values of $\log(R)$ the differences are much smaller (see Fig. 2). When other elements are included (the 'metals') the differences between OP and OPAL are generally much smaller, because in the regions concerned the contributions to opacities from those other elements will generally be much larger than those from H and He. Thus Fig. 1 shows no sign of the discrepancy between OP and OPAL shown in Fig. 2.

8 CARBON AND OXYGEN

For the C and O RM calculations we include in (6) all states ψ_p that belong to the ground complex of the $(N-1)$-electron system, that is to say all states with the same set of principal quantum numbers as the ground state. Thus the system with $N = 6$ electrons has a ground configuration of $1s^2 2s^2 2p^2$ and the ground complex of the $(N-1)$-electron system contains the configurations $1s^2 2s^2 2p$, $1s^2 2s 2p^2$ and $1s^2 2p^3$. With those choices for the ψ_p, all bound states of C and O can be represented by expansions of the type (6). *R*-matrix calculations were made for all bound states with an outer electron having quantum numbers $n\ell$ with $n \leqslant 10$ and $\ell \leqslant$ LMAX with LMAX varying between 2 and 4: states with $\ell >$ LMAX were treated in hydrogenic approximations.

Independent evaluations of OP oscillator strengths for C, N and O have been made in Wiese, Fuhr & Deters (1996). The OP values are found to compare favourably with experimental data and with data from other refined calculations. For most transitions in C, N and O the OP data are recommended in Wiese et al. (1996) as the best available. For C and O, in addition to the *R*-matrix data, we now include data for inner-shell transitions from Badnell & Seaton (2003).

We recall that the OPAL website provides Rosseland-mean opacities for 'metal' mass-fractions $Z \leqslant 0.1$. Figs 5 and 6 compare OP and OPAL opacities for H/C and H/O mixtures with $X = 0.9$ and $Z = 0.1$. Agreement is fairly close.

For the lower temperatures, $\log(T) \lesssim 5.5$, the differences between OP and OPAL may be caused by differences in atomic data, with the OP RM data probably being the more accurate. The maxima at higher temperatures ($\log(T) \simeq 6.0$ for C and 6.2 for O) result from transitions with *K*-shell initial states (electrons with principal quantum number $n = 1$). For the higher densities in those regions, $\log(R) \gtrsim -2$, the opacities from OP are larger than those from OPAL, which is an EOS effect.

In the regions concerned the dominant ionization stages for C and O are H-like and He-like, and for OP dissolution occurs for outer electrons having $n \gtrsim 3$, while for OPAL it occurs at considerably larger values of n; hence OPAL will have more electrons in highly excited states, and less in states with $n = 1$, giving smaller opacities. For the reasons given in Section 3.2 we consider that OP may give the more accurate results for the positions at which dissolution occurs.

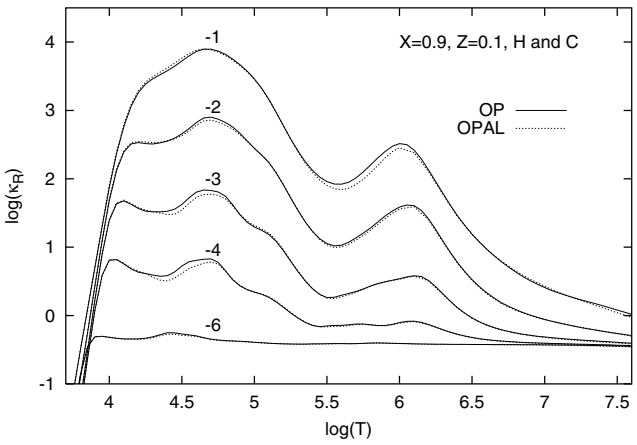

Figure 5. Comparisons of $\log(\kappa_{\rm R})$ from OP and OPAL for a H/C mixture with mass fractions $X = 0.9$ for H and $Z = 0.1$ for C. Curves are labelled by values of $\log(R)$.

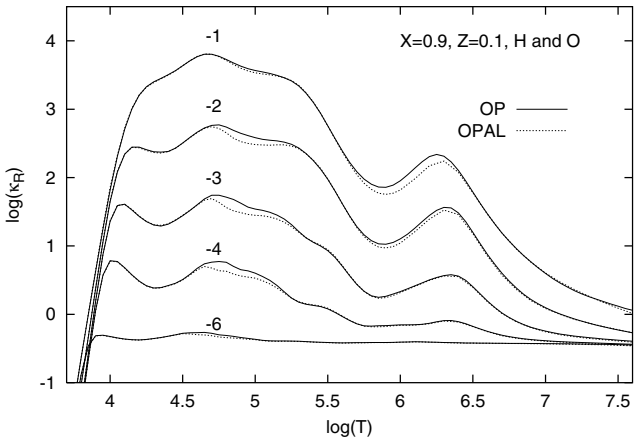

Figure 6. Comparisons of $\log(\kappa_R)$ from OP and OPAL for a H/O mixture with mass fractions $X = 0.9$ for H and $Z = 0.1$ for O. Curves are labelled by values of $\log(R)$.

9 SULPHUR

For ions with numbers of electrons $N \leqslant 11$, the ground complexes for the $(N - 1)$-electron cores contain only 1s, 2s and 2p electrons but for $N > 11$ 3d electrons must also be included and the number of configurations in the complexes can become very large. For such values of N that number was, in general, too large for the inclusion of all such states in the RM expansions and some further approximations were required. Thus even for the case of $N = 13$ the configurations $3s^2$, 3s3p, 3s3d and $3p^2$ were included but 3p3d and $3d^2$ were omitted. For the case of S, with $N \leqslant 16$, such omissions occurred only for the earlier ionization stages where the omitted core states would be rather high and their omission would be unlikely to lead to serious error.

Fig. 7 compares OP and OPAL opacities for an H/S mix with $X = 0.9$ and $Z = 0.1$. The level of accord is similar to that observed for C and O. For S, κ_R(OP) is larger than κ_R(OPAL) at the higher densities in the K-shell region at $\log(T) \simeq 6.7$. That is an EOS effect.

10 IRON

Iron plays a special role in calculations of opacities for typical cosmic mixtures, in consequence of its comparatively high abundance and the very large numbers of lines in its spectra. As the nuclear charge Z increases, all levels in a complex eventually become degenerate (in the limit of $Z \to \infty$ the one-electron energies, when relativistic effects are neglected, depend only on the principal quantum numbers n). With increasing Z the levels in a complex move downward and the number of bound levels in a complex therefore increases. Consider iron with $N = 16$ (Fe XI) which has a ground configuration $3s^2 3p^4$ and a ground complex containing all configurations of the type $3s^x 3p^y 3d^z$ with $x + y + z = 6$. Runs with AS give the number of spectroscopic terms that belong to that complex and have energies below the ionization limit to be equal to 721. There are large numbers of radiative transitions between such states (the '$3 \to 3$' transitions) and from such states (the '$3 \to n$' transitions with $n > 3$). It was first shown in the OPAL work that such transitions in iron ions with $N = 14$ to 19 give rise to an important feature in the Rosseland-mean, at $\log(T) \simeq 5.2$, which has come to be known as the 'Z-bump' (Iglesias, Rogers & Wilson 1987) (see Fig. 1).

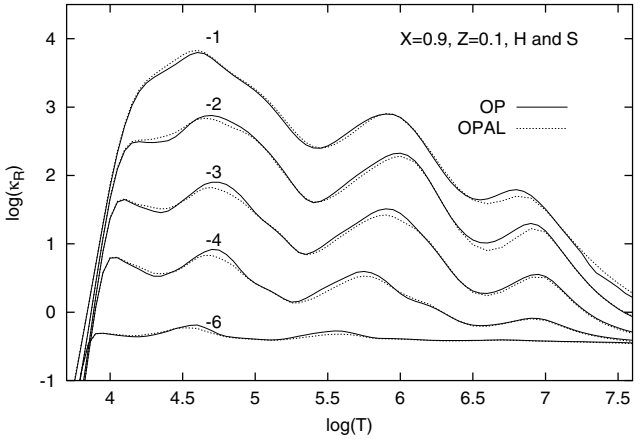

Figure 7. Comparisons of $\log(\kappa_R)$ from OP and OPAL for a H/S mixture with mass fractions $X = 0.9$ for H and $Z = 0.1$ for S. Curves are labelled by values of $\log(R)$.

10.1 Summary of iron data used

Calculations have been made in both LS coupling and in intermediate coupling (IC). Table 3 gives a summary of the atomic data for iron used in various stages of the OP work.

10.1.1 Data from Kurucz

For the first few ionization stages, $N = 21$ to 26, data from Kurucz (1998) were used for nearly 7 million lines. The data were computed using the code of Cowan (1981). The contributions from those stages is not normally of major importance for calculation of the Rosseland means but can be of crucial importance for radiative accelerations (Seaton 1997).

10.1.2 R-matrix calculations

RM calculations for energy levels, oscillator strengths and photoionization cross-sections were made for all ionization stages of iron but for $N = 21$ to 26 only the photoionization data were used (much larger amounts of data being available from Kurucz). In Table 3 the numbers of levels and lines are given separately for $N = 21$ to 26, $N = 14$ to 20 (the region of the Z-bump) and for $N = 2$ to 13. For $N = 2$ to 13 the data from RM are probably the best available.

10.1.3 Use of SUPERSTRUCTURE

The RM method was not capable of providing the very large amounts of data in the region of the Z bump, and further data for over 3 million

Table 3. Atomic data for iron.

N	Method	Coupling	Levels	Lines	PI
21–26	Kurucz	IC	65 427	6 920 198	—
20–26	RM	LS	8 925	368 445	4 479
14–20	RM	LS	6 502	276 450	4 639
2–13	RM	LS	4 232	151 974	3 559
14–19	SS	LS	134 635	3 295 773	2 537
14–19	AS, outer	LS	371 483	4 594 253	8 006
14–19	AS, outer	IC	1 011 266	30 555 846	20 851
2–14	AS, inner	LS	(7 688)*	2 145 442	1 339

*Lower (initial) levels only.

lines were calculated using SS (Lynas-Gray, Storey & Seaton 1995), and used in Seaton et al. (1994).

10.1.4 Inner-shell data from AUTOSTRUCTURE

More recently, inner-shell data from AS, for iron and other elements, have been included (Badnell & Seaton 2003). In that paper it was found that, for inner-shell data, use of IC, in place of LS coupling, did not give any significant change in Rosseland means. Here we consider only LS coupling inner-shell data.

10.1.5 Further data from AUTOSTRUCTURE

In the present paper we consider the replacement of data from RM and SS, in the regions of the Z-bump ($N = 14$ to 19), with further outer-shell data from AS. Calculations were made using both LS coupling and IC with over 30 million lines for the latter case.

10.1.6 Photoionization

The numbers given under the heading 'PI' in Table 3 correspond to the numbers of initial states for which photoionization cross-sections were calculated: each cross-section contains data for all available final states.

10.2 Use of new AS data in LS coupling

For ionization stages giving the Z bump, $N = 14$ to 19, we tried replacing all old (RM plus SS) data with the new AS data in LS coupling. We obtained Rosseland means close to those from the original OP work, which provided a good independent check. The only significant differences were in fairly restricted regions where photoionization had been estimated using SS data (the SS estimates were rather crude – see Lynas-Gray et al. 1995).

10.3 Intercombination lines

We replaced all old (RM plus SS) data for $N = 14$ to 19 with new AS data in IC. The differences with Rosseland means from the previous subsection (AS data in LS coupling) was almost entirely owing to inclusion of the intercombination lines in AS. Fig. 8 shows the percentage increase in the mean that results from inclusion of the intercombination lines [up to 18 per cent for $\log(R) = -4$]. The inclusion of those lines gives improved agreement with OPAL near the maximum of the Z-bump. On a log–log scale, however, our final results for the six-element mix do not appear greatly different to the eye from those shown in Fig. 1.

10.4 Many-electron jumps

Selection rules state that radiative transitions can occur only between configurations that differ in the states of one electron. In CI calculations the states may be given configuration labels but transitions can occur between states having configuration labels differing by more than one electron (the 'many-electron jumps'). The effect can be a further redistribution of oscillator strength. We have made runs in which the many electron jumps are omitted. Fig. 9 shows the percentage increase which results from inclusion of those jumps. The effect is not large (no more than 8 per cent). It is not included by OPAL.

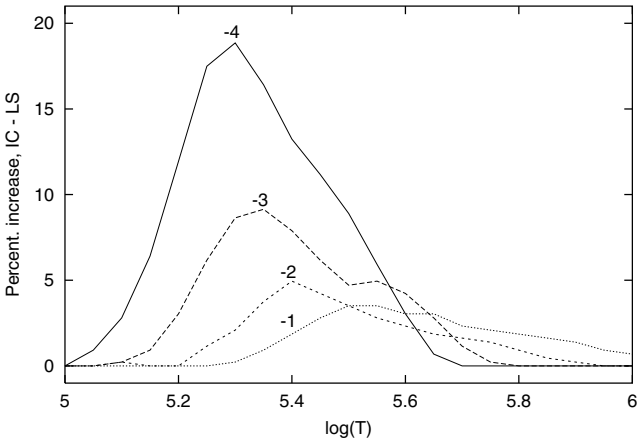

Figure 8. Percentage increase in $\kappa_{\rm R}$, for the six-element mix, which results from the inclusion of iron intercombination lines. Curves are labelled by values of $\log(R)$.

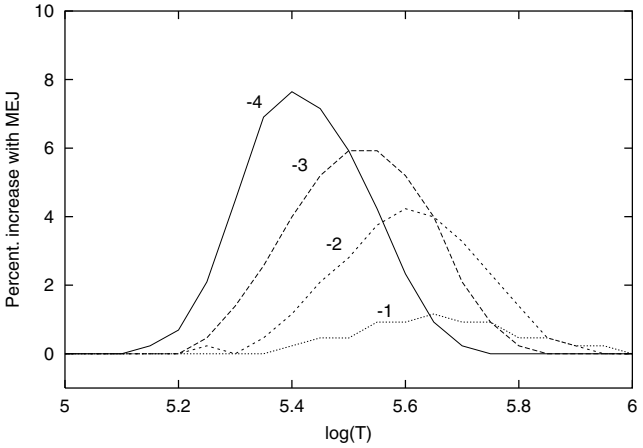

Figure 9. Percentage increase in $\kappa_{\rm R}$, for the six-element mix, which results from the inclusion of iron many-electron-jumps (MEJ). Curves are labelled by values of $\log(R)$.

10.5 Results for an iron-rich mixture

It has already been noted that the OPAL website cannot provide opacities for mixtures with $Z > 0.1$. A further restriction is that it cannot provide data for cases in which Z is pure iron (that restriction arises because such cases can be very sensitive to behaviour near minima in the iron monochromatic opacities). About the most iron-rich case for which we can obtain OPAL data is $X = 0.9$, $Z = 0.1$ and Z containing C and Fe in the ratio of 2:1 by number fraction.

Fig. 10 compares OP with OPAL for the iron-rich mixture.

At low densities inclusion of iron intercombination transitions in the OP work lead to an increase in $\kappa_{\rm R}$ in the region of the maximum of the Z-bump, giving close agreement between OP and OPAL in that region. But the position of the Z-bump given by OP is shifted to slightly higher temperatures, compared with OPAL.

At higher densities there are some differences between the OP and OPAL results shown on Fig. 10. At those densities there are some suggestions of rather irregular variations in the OPAL data which might be caused by interpolation errors near the edges of the domain of validity for the OPAL interpolations.

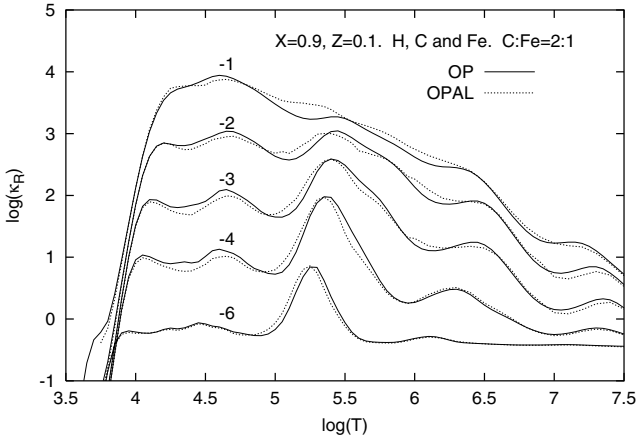

Figure 10. Comparisons of $\log(\kappa_R)$ from OP and OPAL for an iron-rich mixture: $X = 0.9$, $Z = 0.1$ and C:Fe=2:1 by number fraction. Curves are labelled by values of $\log(R)$.

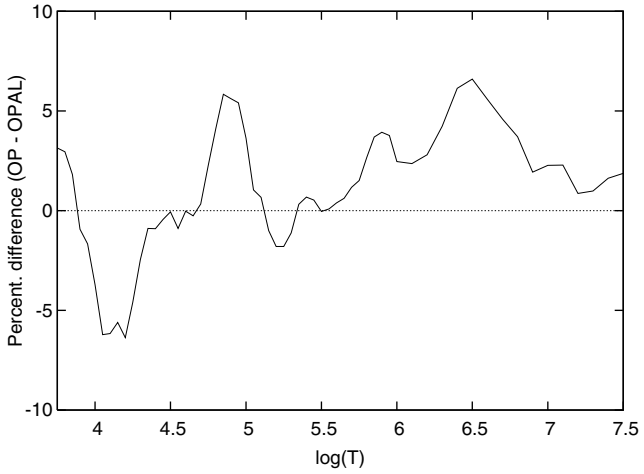

Figure 11. Percentage differences, (OP – OPAL), between κ_R for the six-element mix at $\log(R) = -1.5$.

11 THE SOLAR RADIATIVE INTERIOR

Computed solar models are sensitive to radiative opacities in the solar radiative interior, the region below the base of the solar convective zone at R_{CZ}. It is shown in two recent papers (Basu & Antia 2004; Bahcall et al. 2004) that helioseismology provides remarkably accurate measures of R_{CZ}, and hence stringent tests of the accuracy of solar models. In those papers it is noted that recent work leads to revisions in solar element abundances and that, when those revisions are taken into account, there are significant differences between values of R_{CZ} obtained from helioseismology measurements and from solar models calculated using OPAL opacities. In Basu & Antia (2004), from a study using envelope models, it is argued that in order to obtain a correct density profile it is necessary to adopt opacities at R_{CZ} larger than those from OPAL by an amount of 19 per cent; while in Bahcall et al. (2004), from a study of full evolution models, it is found that an increase by 21 per cent is required.

At R_{CZ} the best estimates (Bahcall et al. 2004) of the temperature and density are $\log(T) = 6.338$ and $\log(\rho) = -0.735$, giving $\log(R) = -1.75$. In Fig. 11 we show the percentage differences (OP – OPAL) in κ_R against $\log(T)$ for the six-element mix at $\log(R) = -1.75$. At $\log(T) = 6.338$ we find κ_R(OP) to be larger than κ_R(OPAL) by 5.0 per cent, which is much less than the change required in Basu & Antia (2004) and Bahcall et al. (2004). We believe it to be highly unlikely that the opacities can be increased to the values required by Basu & Antia (2004) and Bahcall et al. (2004).

12 SUMMARY

There are two main steps in opacity calculations.

(i) *The EOS problem*, determination of the populations of all species in a plasma, which can lead to absorption of radiation.

(ii) *The atomic physics problem*, obtaining the atomic data that control the efficiencies of the the radiative processes.

12.1 The EOS problem

The OPAL and OP approaches to the EOS problem are very different (see Section 3).

We encounter two cases for which differences between OP and OPAL opacities are due to different treatments of the EOS problem.

The first is for $\log(R) \simeq -1$ and $\log(T) \simeq 6.0$ for H and 6.4 for He (see Section 3). For those cases OP gives the ground states of H^0 and He^+ to be undergoing dissolution, leading to pressure ionization, while OPAL has much larger populations for those states. The biggest difference is for He at $\log(T) \simeq 6.4$ and $\log(R) = -1$, for which κ_R(OPAL) is larger than κ_R(OP) by 20 per cent. We are not aware of any experimental or observational evidence in favour of one result or the other.

The second case concerns K-shell transitions in 'metals' at the higher densities, where OPAL has larger populations in excited states, and hence less in states with $n = 1$ giving smaller opacities. That causes the 5 per cent difference between κ_R(OP) and κ_R(OPAL) at conditions corresponding to those at the base of the solar convective zone (see Section 11).

12.2 Atomic data

It is essential to consider both the quantity and the quality of the atomic data used.

The OP work was started, a little over 20 years ago, with the ambitious intention of computing all of the required atomic data using the sophisticated R-matrix method, RM. The OPAL work was started, at about the same time, with the less ambitious approach of using single-configuration wavefunctions computed with the aid of parametric potentials adjusted empirically so as to give best agreement with experimental energies. The OPAL work quickly led to the discovery of the Z-bump, a feature at $\log(T) \simeq 5.2$ produced by a very large number of iron lines. OP was unable to compute data for such large numbers of lines using the RM method, but was able to make supplementary computations using the code SUPERSTRUCTURE which includes some allowance for CI effects. The first published OP opacities had substantial differences from OPAL only at rather high temperature and densities and in Iglesias & Rogers (1996) it was suggested that OP was missing some data for inner-shell transitions. That suggestion is confirmed as correct in our recent paper (Badnell & Seaton 2003). The RM and SS codes are both unsuitable for handling the inner shell processes and we therefore used the code AUTOSTRUCTURE (AS). In the present paper we also include a large amount of outer-shell data from AS.

13 CONCLUSIONS

Our main conclusion is that there is good general agreement between OP and OPAL opacities for the six elements H, He, C, O, S and Fe. We expect to obtain equally good agreement for other elements once work is complete on the calculation of further inner-shell data.

There are some indications that the OPAL interpolation procedures described in Rogers & Iglesias (1993) may introduce some errors near the edges of the domains of validity that are claimed.

At lower temperatures, $\log(T) \lesssim 5.5$, there are some modest differences between OP and OPAL which may be a consequence of the greater sophistication of the OP atomic-data work. At higher temperatures and higher densities, $\log(R) \gtrsim -2$, the OP opacities tend to be larger than those from OPAL in consequence of the use of different equations of state.

ACKNOWLEDGMENTS

We thank Drs F. J. Rogers and C. A. Iglesias for their friendly comments on the present work. We also thank Drs H. M. Antia, J. N. Bahcall and F. Delahaye for their helpful comments.

REFERENCES

Badnell N. R., 1987, J. Phys. B, 19, 3827
Badnell N. R., 1997, J. Phys. B, 30, 1
Badnell N. R., Seaton M. J., 2003, J. Phys. B, 36, 4367
Bahcall J. N., Serenelli A. M., Pinsonneault M., 2004, ApJ, submitted (astro-ph/0403604)
Basu S., Antia H. M., 2004, ApJ, 606, L85
Berrington K. A., Burke P. G., Butler K., Seaton M. J., Storey P. J., Taylor K. T., Yu Yan, 1987, J. Phys. B, 20, 6379
Burke V. M., 1992, J. Phys. B, 25, 4917
Cowan R. D., 1981, The Theory of Atomic Structure and Spectra. Univ. California Press, Berkeley, CA
Dimitrijević M. S., Konjević N. S., 1981, in Wende B., ed., Spectral Line Shapes. de Gruyter, Berlin, p. 211
Eissner W., Jones M., Nussbaumer H., 1974, Comp. Phys. Comm., 8, 270
Graboske H. C., Harwood D. C., Rogers F. J., 1969, Phys. Rev., 186, 210
Griem H. R., 1968, Phys. Rev., 165, 258
Hummer D. G., 1988, AIP Conf. Proc., 168, 1
Hummer D. G., Mihalas D., 1988, ApJ, 331, 794
Iglesias C. A., Rogers F. J., 1996, ApJ, 464, 943
Iglesias C. A., Rogers F. J., Wilson B. G., 1987, ApJ, 322, L45
Iglesias C. A., Rogers F. J., Wilson B. G., 1992, ApJ, 397, 717
Kurucz R. L., 1988, in McNally D., ed., Trans. IAU XXB. Kluwer, Dordrecht, p. 168
Lynas-Gray A. E., Storey P. J., Seaton M. J., 1995, J. Phys. B, 28, 2817
Nayfonov A., Däppen W., Hummer D. G., Mihalas D., 1999, ApJ, 526, 451
Rogers F. J., 1981, Phys. Rev. A, 23, 1008
Rogers F. J., Iglesias C. A., 1992a, ApJS, 79, 507
Rogers F. J., Iglesias C. A., 1992b, Rev. Mex. Astron. Astrofis., 23, 133
Rogers F. J., Iglesias C. A., 1993, ApJ, 401, 361
Rogers F. J., Wilson B. G., Iglesias C. A., 1988, Phys. Rev. A, 38, 5007
Seaton M. J., 1987a, J. Phys. B, 20, 6363
Seaton M. J., 1987b, J. Phys. B, 20, 6431
Seaton M. J., 1988, J. Phys. B, 21, 3033
Seaton M. J., 1993, MNRAS, 265, L25
Seaton M. J., 1997, MNRAS, 289, 700
Seaton M. J., Zeippen C. J., Tully J. A., Pradhan A. K., Mendoza C., Hibbert A., Berrington K. A., 1992, Rev. Mex. Astron. Astrofis., 23, 19
Seaton M. J., Yu Yan, Mihalas D., Pradhan A. K., 1994, MNRAS, 266, 805
The Opacity Project Team, 1995, The Opacity Project Vol. 1 IOP Publishing, Bristol
The Opacity Project Team, 1997, The Opacity Project Vol. 2. IOP Publishing, Bristol
Wiese W. L., Fuhr J. R., Deters T. M., 1996, Atomic Transition Probabilities for Carbon, Nitrogen and Oxygen: A Critical Compilation. J. Phys. Chem. Ref. Data, Monograph 7

This paper has been typeset from a TEX/LATEX file prepared by the author.